

Label-Free Detection of Micro-RNA Hybridization Using Surface-Enhanced Raman Spectroscopy and Least-Squares Analysis

Justin L. Abell,^{*,†} Jeonifer M. Garren,[‡] Jeremy D. Driskell,[§] Ralph A. Tripp,^{||} and Yiping Zhao[⊥]

[†]Department of Biological and Agricultural Engineering, University of Georgia, Athens, Georgia 30602, United States

[‡]Department of Biostatistics and Epidemiology, Georgia Health Science University, Augusta, Georgia 30912, United States

[§]Department of Chemistry, Illinois State University, Normal, Illinois 61790, United States

^{||}Department of Infectious Diseases, University of Georgia, Athens, Georgia 30602, United States

[⊥]Department of Physics and Astronomy, University of Georgia, Athens, Georgia 30602, United States

Supporting Information

ABSTRACT: Label-free surface-enhanced Raman spectroscopy (SERS) detection of nucleic acid hybridization is impeded by poor spectral reproducibility and the fact that the chemical signatures of hybridized and unhybridized sequences are highly similar. To overcome these issues, highly reproducible silver nanorod SERS substrates along with a straightforward least-squares (LS) technique have been employed for the quantitative determination of the relative ratios of the four nucleotide components A, C, G, and T/U before and after hybridization using a clinically relevant micro-RNA sequence.

Nucleic acid detection is indispensable for genomic screening or monitoring of pathogenic and cellular activity. Traditionally, this detection has relied almost exclusively on polymerase chain reaction (PCR) and DNA microarray techniques.^{1,2} However, these methods require extrinsic labels (e.g., fluorophores or radiolabels) for detection of probe–target hybridization, which ultimately increases the cost and complexity of the detection assay. To address this issue, label-free techniques such as surface plasmon resonance (SPR) have been investigated,³ but these methods detect only changes in mass and do not provide a chemical-specific readout.

As a highly sensitive and chemical-specific label-free detection technique, surface-enhanced Raman scattering (SERS) offers a potential alternative.^{4–7} For example, previous reports have shown that spectral features change upon hybridization^{4,5,7} and that relative peak intensities due to A and C can be quantified.⁶ However, to date, label-free SERS detection of hybridization has lacked spectral detail, reproducibility, and/or a means of statistical analysis for quantitative analysis. This is due to several important issues. For one, SERS has traditionally suffered from poor spectral reproducibility. However, we have previously demonstrated that silver nanorod (AgNR) substrates demonstrate excellent reproducibility for SERS measurements (~10% relative standard deviation)^{8,9} and have been successfully employed for quantitative DNA detection.^{10,11} Second, the target–probe duplex is composed of the same four nucleotide components as the probe sequence, and therefore, the SERS signals before and after hybridization are very similar. One method that can be used to discriminate

among highly similar SERS spectra is to use multivariate statistical approaches such as principal component analysis (PCA) or partial least-squares (PLS).^{10,11} In the current report, we propose the use of SERS in conjunction with a straightforward least-squares (LS) regression approach for quantitative determination of the composition of heterogeneous DNA probe sequences immobilized on the surface AgNR substrates. The LS method was previously adopted by Prado et al.¹² to decipher the physical ratios of pure homogeneous nucleotide sequences within a mixture of sequences using SERS. In addition, we monitor the change in the composition after hybridization with complementary micro-RNA (miRNA) target sequences. We show that this approach is a simple and valid method for direct, label-free DNA hybridization detection.

Our hypothesis is that for a given heterogeneous DNA sequence, the SERS signal (S_{DNA}) is a linear combination of the individual A, C, G, and T nucleotide signals (S_A , S_C , S_G , and S_T , respectively). Therefore, $S_{\text{DNA}} = aS_A + cS_C + gS_G + tS_T$, where a , c , g , and t represent the relative contribution of each source and directly reflect the physical quantity of A, C, G, and T immobilized on the surface. If the functional groups A, C, G, and T have the same enhancement, then a , c , g , and t will be directly proportional to the numbers of the corresponding nucleotides in the DNA sequence. Upon hybridization, the ratios of these coefficients will change according to the complementary nature of DNA, which dictates that $a = t$ and $c = g$ for a completely complementary hybridized sequence. Thus, a linear LS regression algorithm can be used to estimate these coefficients and therefore determine the relative numbers of nucleotides present within a DNA sequence before and after hybridization. We demonstrate the feasibility of this strategy using four different 5'-thiol-modified single-stranded DNA probes, labeled as let-7f, Test, miR-224, and reverse (rev) let-7f, each of which contains a different A:C:G:T ratio and/or sequence [Table S1 in the Supporting Information (SI)]. To allow for reproducible, efficient, and parallel screening of multiple samples, we employ an array-patterned 40-well AgNR SERS chip.¹³ Figure 1 shows the measured SERS spectra of the immobilized probes. The spectra of the pure RNA mono-

Received: May 4, 2012

Published: July 12, 2012

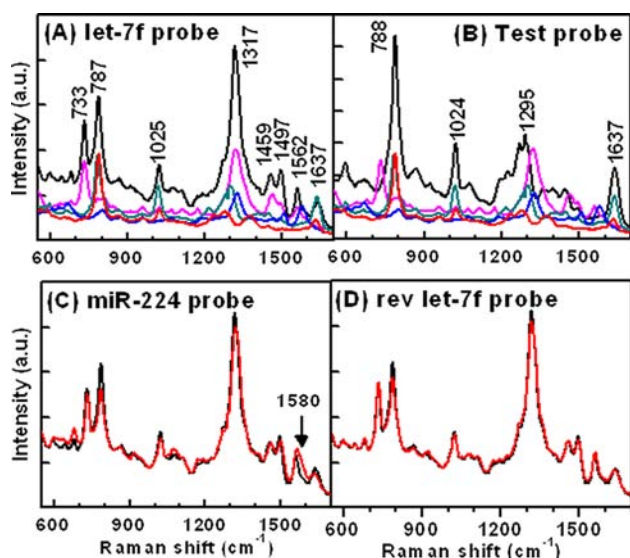


Figure 1. SERS spectra of DNA probes: (A) let-7f; (B) Test; (C) miR-224; (D) rev let-7f. In (A) and (B), the probe spectra are shown in black and the spectra of the pure mononucleotides (scaled for comparison) in color: pink = AMP, green = CMP, blue = GMP, red = UMP. In (C) and (D), the normalized probe spectra are shown in red, with the let-7f probe spectrum shown in black for comparison.

nucleotides are plotted as references (see Figure S1 in the SI for more detailed spectra).

The SERS spectrum of let-7f (Figure 1A) has most of the spectral features of the pure A, C, and U nucleotides. All of the band assignments are based on those found in the literature.^{14,15} These include 733 cm^{-1} (A, ring-breathing), 788 cm^{-1} (C and T, ring-breathing), and 1317 cm^{-1} (A, ring-stretching) bands. We point out that DNA contains T rather than U. However, the spectra of these two analogues are very similar (see the SI). The Test probe is a synthetic sequence composed of only C and T in an alternating manner. Concordantly, the 733 and 1317 cm^{-1} bands of A are absent, but the spectrum retains a strong band at 788 cm^{-1} , which is most likely a convolution of the C and T ring-breathing modes found at 783 and ~ 795 cm^{-1} , respectively (Figure 1B). The miR-224 probe (Figure 1C) contains all four nucleotides, and the spectrum is very similar to that of the let-7f probe, with only a subtle decrease in the relative intensities of the 733, 788, and 1317 cm^{-1} bands. The 1560 cm^{-1} band shows increased intensity and significant right-sided broadening, presumably as a result of the presence of the nearby G band at 1580 cm^{-1} . The rev let-7f probe is the reverse sequence of the let-7f probe. Hence, its spectrum (Figure 1D) is extremely similar to that of let-7f, with very subtle differences in the intensities of the most prominent bands at 733, 788, and 1317 cm^{-1} .

Figure 2 shows the coefficients a , c , g , and u (i.e., t) extracted by LS for the four DNA probes and their comparison to the theoretical A:C:G:T ratios determined by the physical composition (pink stars). These results were acquired only after removing portions of the spectrum around the 1317 cm^{-1} peak (see the SI for a detailed discussion). The g and u values are very close to the theoretical values, whereas the a and c values are over- and underestimated, respectively, by approximately ± 0.15 . These results validate our hypothesis that the LS-SERS method is feasible for quantitative compositional analysis of ssDNA.

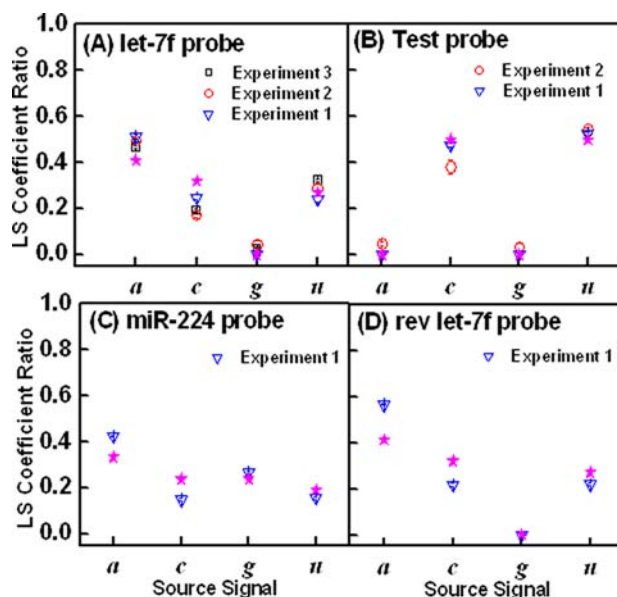


Figure 2. LS-estimated coefficients a , c , g , and u from the measured probe spectra: (A) let-7f; (B) Test; (C) miR-224; (D) rev let-7f. Error bars show the standard deviations of replicates within each experiment. (A) and (B) include the fits from replicate experiments for comparison. The pink stars represent the theoretical values.

miRNA target sequences were then incubated with the immobilized probes after the probes had been pretreated with mercaptohexanol (MCH) spacer (Figure S5; see the SI for a detailed discussion).¹⁶ All four probes were treated with the let-7f, Test, and rev miR-224 miRNA targets as well as saline sodium citrate (SSC) buffer alone as a control. The let-7f target is complementary to the let-7f probe and is a clinically relevant sequence that plays a role in cellular differentiation and tumor suppression.¹⁷ The Test target is an artificial sequence complementary to the Test probe. The rev miR-224 target sequence is the reverse of the real miR-224 sequence, and this target is therefore noncomplementary to the miR-224 probe.

Figure 3A shows the normalized spectra of the let-7f probe treated with the noncomplementary rev miR-224 target and the SSC control, which appear to be essentially identical. This would be expected if we assume that the probe treated with a noncomplementary miRNA target maintains the same nucleotide ratios as that treated with no target. When the let-7f probe was treated with noncomplementary Test target, however, a subtle increase in the relative intensity of the 1317 cm^{-1} peak could be seen in addition to some slight spectral deviations from the other two negative controls, which could result from cross-hybridization. For the let-7f probe treated with the complementary let-7f target, we would expect to see the appearance of the G band at 1580 cm^{-1} after hybridization with the G-containing complementary target, or at least a broadening of the 1560 cm^{-1} band (see Figure 1C). However, the 1560 cm^{-1} band appeared to broaden in all of the let-7f probe samples regardless of the hybridization treatment. On the other hand, the intensity did not appear to have increased, so we suspect that this spectral feature could be a result of reorientation of the probe rather than the presence of G.¹⁸

The Test probe demonstrated more obvious spectral changes when treated with the complementary Test target. The appearance of the 733 cm^{-1} band and the increased intensity and shifting of the 1300 cm^{-1} band toward 1317 cm^{-1} are

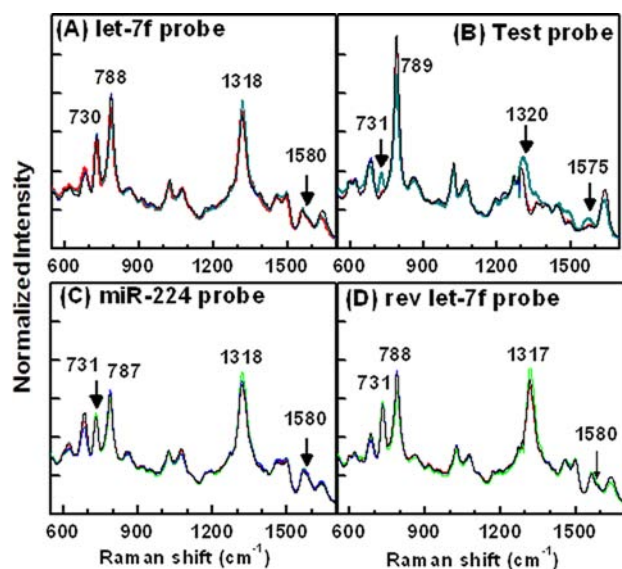


Figure 3. Normalized spectra of the (A) let-7f, (B) Test, (C) miR-224, and (D) rev let-7f probes after treatment with the targets let-7f (red), Test (green), and rev miR-224 (blue) or the SSC buffer control (black).

indicative of the presence of A. Moreover, the 1580 cm^{-1} band appeared, indicating the presence of G. All three of the negative control treatments showed identical spectra, suggesting minimal cross-hybridization.

The miR-224 and rev let-7f probes were treated only with negative controls; likewise, the resulting spectra are virtually identical. However, the spectra for the Test target treatment demonstrate subtle differences relative to the other negative controls, such as a notable increase in the 1317 cm^{-1} band. These observations reassert that the Test target has a higher likelihood of cross-hybridizing with noncomplementary probes.

Clearly the spectral differences between the complementary and noncomplementary hybridizations are subtle. To confirm that the let-7f target selectively hybridized to the let-7f probe, we used a let-7f target labeled at its 5' end with the surface-enhanced resonance Raman spectroscopy (SERRS) label FAM (Figure S6). Indeed, only the let-7f probe demonstrated a significant FAM signal, confirming that the let-7f target indeed hybridized with the let-7f probe and did not cross-hybridize with other probes.

LS was performed to estimate a , c , g , and u for the let-7f and Test probe spectra after treatment with complementary and noncomplementary targets (Figure 4). The theoretical values based on completely hybridized sequences are shown for comparison as pink stars. After hybridization of the let-7f probe, a , c , g , and u were expected to be 0.34, 0.16, 0.16, and 0.34, respectively. Figure 4A shows that the LS estimates of c and u are close to the theoretical hybridization values, but some discrepancies exist for a and g , which were estimated to be 0.42 and 0.08, respectively. This is likely due to incomplete hybridization. Furthermore, in Figure 4B, the estimated LS ratios of the negative controls yield values fairly close to the theoretical ratios for the let-7f probe.

For complete complementary hybridization of the Test probe, the theoretical a , c , g , and u values all equal 0.25. However, in Figure 4C, the estimated values of both a and g (0.15 and 0.13, respectively) are noticeably less than the theoretical values, while $u = 0.5$ is noticeably higher. The

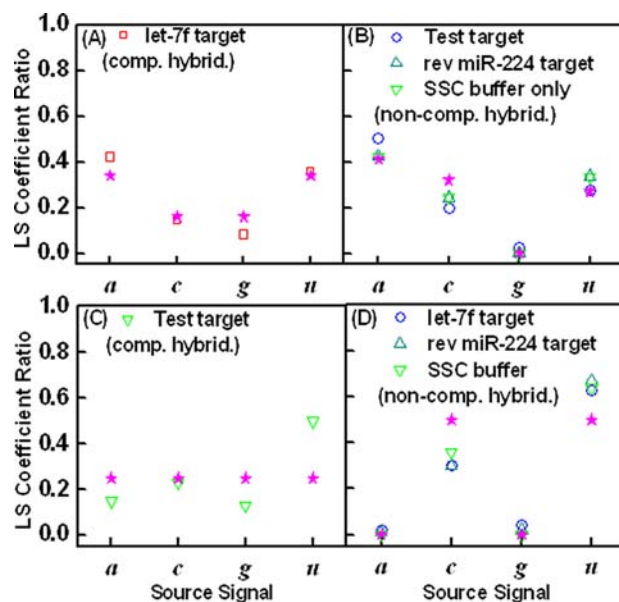


Figure 4. Estimated LS coefficient ratios of (A, B) the let-7f probe hybridized with (A) the let-7f target and (B) negative controls and (C, D) the Test probe hybridized with (C) the Test target and (D) negative controls. The pink stars represent the theoretical ratios.

discrepancies between the theoretical and estimated values could be a result of incomplete hybridization. This idea is corroborated by the spectrum shown in Figure 3B, where we can see only weak A and G signals relative to C and U. With 100% hybridization of the Test probe, we would expect the resulting spectrum to resemble that of the miR-224 probe in Figure 1C, which shows a significant contribution from A. For the three negative controls (Figure 4D), a and g are very close to the theoretical values of zero, but the c and u values appear to be under- and overcompensated by approximately 0.2, respectively. Compared with the negative controls, the estimated a , c , g , and u values for complementary hybridization are indeed much closer to the theoretical values, which unambiguously demonstrates hybridization.

In Figure 4, we compare the estimated LS coefficients after hybridization with the theoretical ratios predicted with 100% hybridization efficiency. Since established hybridization-based detection techniques such as DNA microarrays typically achieve a hybridization efficiency of $\sim 50\%$,³ we may expect incomplete hybridization on the AgNRs as well. However, this should not be a major issue for the LS method, as intermediate degrees of hybridization should be captured by the LS fitting. To evaluate this notion, we performed a concentration-dependent analysis of the let-7f target. Figure 5 shows that as the concentration of the target increases, the relative ratios of a and c steadily decrease, while the complements g and u steadily increase. This is to be expected on the basis of the fact that after complete hybridization $a = u$ and $c = g$, that is, the values should converge. The dashed lines in Figure 5 represent the theoretical limits to which the values should converge assuming 100% hybridization. The solid lines show estimates of the actual values to which the ratios converged, which are offset from the theoretical values by approximately -0.07 and $+0.07$ for c/g and a/u , respectively. We also note that the a and u values estimated for zero concentration (i.e., SSC buffer only, plotted at $1 \times 10^{-3}\ \mu\text{M}$) appear to be under- and overcompensated, respectively, in comparison with the other values of the

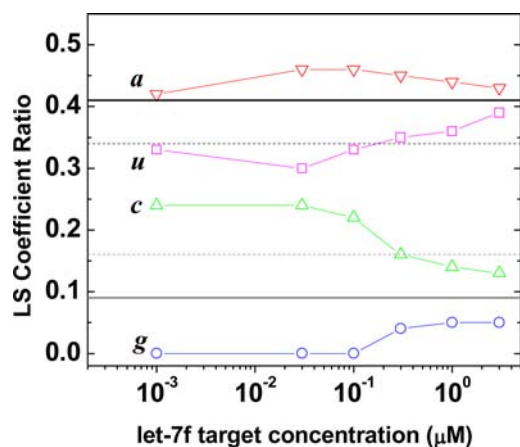


Figure 5. Log plots of the estimated LS coefficient ratios as functions of the let-7f target concentration. The solid horizontal lines show the estimated convergence values for *c* and *g* (black) and *a* and *u* (gray). The corresponding dashed lines show the theoretical values of the ratios assuming 100% hybridization. The coefficient ratios estimated for 0 μM (SSC only) are plotted at 0.001 μM as a reference.

calibration curve. The exact reason for this is unclear, but it could be due to a lack of optimized experimental processing (e.g., rinsing step) or data preprocessing (e.g., removing spectral regions that contribute to inaccurate LS fitting).

In this communication, we have shown conclusively for the first time that LS and SERS can be integrated together (i) to determine directly the composition ratios of probes immobilized onto the AgNRs and (ii) to capture subtle changes in the spectra resulting from label-free hybridization, at least semi-quantitatively, by a straightforward LS analysis. Clearly, room for improvement exists, but we believe that this study highlights a potentially powerful advancement for miRNA label-free hybridization analysis. We also believe that optimization of the hybridization conditions, improved preprocessing of the spectral data, refinement of the LS algorithm, and further investigation of other factors such as the SERS distance dependence could further improve the accuracy of this approach. We intend to investigate these factors further in a future publication.

■ ASSOCIATED CONTENT

📄 Supporting Information

Experimental procedures, pure mononucleotide source SERS spectra, table of DNA and miRNA nucleotide sequences ratios, LS coefficient ratios estimated for DNA probes using the entire spectral region between 350 and 1800 cm^{-1} , reconstructed and difference spectra, MCH spacer SERS spectrum, and FAM-let-7f SERRS spectra. This material is available free of charge via the Internet at <http://pubs.acs.org>.

■ AUTHOR INFORMATION

Corresponding Author

jabell@uga.edu

Notes

The authors declare no competing financial interest.

■ ACKNOWLEDGMENTS

This work was supported by CSREES Grant 2009-35603-0551 and NSF Grant CBET-1064228. J.L.A. thanks Pierre Negri for

helpful conversations regarding DNA immobilization and hybridization and Matthew Ritz for his software expertise.

■ REFERENCES

- (1) Yang, S.; Rothman, R. E. *Lancet Infect. Dis.* **2004**, *4*, 337.
- (2) Git, A.; Dvinge, H.; Salmon-Divon, M.; Osborne, M.; Kutter, C.; Hadfield, J.; Bertone, P.; Caldas, C. *RNA* **2001**, *16*, 991.
- (3) Peterson, A. W.; Heaton, R. J.; Georgiadis, R. M. *Nucleic Acids Res.* **2001**, *29*, 5163.
- (4) Dong, L. Q.; Zhou, J. Z.; Wu, L. L.; Dong, P.; Lin, Z. H. *Chem. Phys. Lett.* **2002**, *354*, 458.
- (5) Barhoumi, A.; Halas, N. J. *J. Am. Chem. Soc.* **2010**, *132*, 12792.
- (6) Green, M.; Liu, F. M.; Cohen, L.; Kollensperger, P.; Cass, T. *Faraday Discuss.* **2006**, *132*, 269.
- (7) Papadopoulou, E.; Bell, S. E. J. *Chem. Commun.* **2011**, *47*, 10966.
- (8) Driskell, J. D.; Shanmukh, S.; Liu, Y.; Chaney, S. B.; Tang, X. J.; Zhao, Y. P.; Dluhy, R. A. *J. Phys. Chem. C* **2008**, *112*, 895.
- (9) Abell, J. L.; Garren, J. M.; Zhao, Y. P. *Appl. Spectrosc.* **2011**, *65*, 734.
- (10) Driskell, J. D.; Seto, A. G.; Jones, L. P.; Jokela, S.; Dluhy, R. A.; Zhao, Y. P.; Tripp, R. A. *Biosens. Bioelectron.* **2008**, *24*, 917.
- (11) Driskell, J. D.; Primera-Pedrozo, O. M.; Dluhy, R. A.; Zhao, Y. P.; Tripp, R. A. *Appl. Spectrosc.* **2009**, *63*, 1107.
- (12) Prado, E.; Daugey, N.; Plumet, S.; Servant, L.; Lecomte, S. *Chem. Commun.* **2011**, *47*, 7425.
- (13) Abell, J. L.; Driskell, J. D.; Dluhy, R. A.; Tripp, R. A.; Zhao, Y. P. *Biosens. Bioelectron.* **2009**, *24*, 3663.
- (14) Bell, S. E. J.; Sirimuthu, N. M. S. *J. Am. Chem. Soc.* **2006**, *128*, 15580.
- (15) Otto, C.; Vandentweel, T. J. J.; Demul, F. F. M.; Greve, J. J. *Raman Spectrosc.* **1986**, *17*, 289.
- (16) Herne, T. M.; Tarlov, M. J. *J. Am. Chem. Soc.* **1997**, *119*, 8916.
- (17) Roush, S.; Slack, F. J. *Trends Cell Biol.* **2008**, *18*, 505.
- (18) Papadopoulou, E.; Bell, S. E. J. *J. Phys. Chem. C* **2011**, *115*, 14228.